

## LETTER

## C<sub>4</sub> anatomy can evolve via a single developmental change

Marjorie R. Lundgren,<sup>1†</sup>  
 Luke T. Dunning,<sup>1</sup> Jill K. Olofsson,<sup>1</sup>  
 Jose J. Moreno-Villena,<sup>1</sup>  
 Jacques W. Bouvier,<sup>1</sup> Tammy L.  
 Sage,<sup>2</sup> Roxana Khoshravesh,<sup>2</sup>  
 Stefanie Sultmanis,<sup>2</sup> Matt Stata,<sup>2</sup>  
 Brad S. Ripley,<sup>3</sup> Maria S.  
 Vorontsova,<sup>4</sup>  
 Guillaume Besnard,<sup>5</sup> Claire Adams,<sup>3</sup>  
 Nicholas Cuff,<sup>6</sup> Anthony Mapaura,<sup>7</sup>  
 Matheus E. Bianconi,<sup>1</sup>  
 Christine M. Long,<sup>8</sup>  
 Pascal-Antoine Christin<sup>1</sup> and  
 Colin P. Osborne<sup>1\*</sup>

### Abstract

C<sub>4</sub> photosynthesis is a complex trait that boosts productivity in warm environments. Paradoxically, it evolved independently in numerous plant lineages, despite requiring specialised leaf anatomy. The anatomical modifications underlying C<sub>4</sub> evolution have previously been evaluated through interspecific comparisons, which capture numerous changes besides those needed for C<sub>4</sub> functionality. Here, we quantify the anatomical changes accompanying the transition between non-C<sub>4</sub> and C<sub>4</sub> phenotypes by sampling widely across the continuum of leaf anatomical traits in the grass *Alloteropsis semialata*. Within this species, the only trait that is shared among and specific to C<sub>4</sub> individuals is an increase in vein density, driven specifically by minor vein development that yields multiple secondary effects facilitating C<sub>4</sub> function. For species with the necessary anatomical preconditions, developmental proliferation of veins can therefore be sufficient to produce a functional C<sub>4</sub> leaf anatomy, creating an evolutionary entry point to complex C<sub>4</sub> syndromes that can become more specialised.

### Keywords

*Alloteropsis*, bundle sheath, C<sub>3</sub>-C<sub>4</sub> intermediate, C<sub>4</sub> photosynthesis, evolution, grass, leaf anatomy, mesophyll, vein density.

Ecology Letters (2019) 22: 302–312

### INTRODUCTION

The vast majority of plants use C<sub>3</sub> photosynthesis, but some lineages evolved the C<sub>4</sub> pathway to overcome environmentally induced limitations on carbon fixation (Ehleringer *et al.* 1991; Sage *et al.* 2011). Net carbon fixation by C<sub>3</sub> photosynthesis is decreased in warm, high light, arid and saline environments that lower CO<sub>2</sub> concentrations within the leaf and increase photorespiration, the process initiated when O<sub>2</sub> instead of CO<sub>2</sub> is fixed by the enzyme Rubisco (Chollet & Ogren 1975). To circumvent the losses of carbon and energy caused by photorespiration, the C<sub>4</sub> pathway spatially separates the initial fixation of carbon and its assimilation by Rubisco across two leaf compartments, thereby concentrating CO<sub>2</sub> at the enzyme's active site to promote CO<sub>2</sub> rather than O<sub>2</sub> fixation (Downton & Tregunna 1968; Hatch 1976). A number of anatomical and biochemical functions must work in concert to sustain the high fluxes of the C<sub>4</sub> cycle, and comparisons of average C<sub>4</sub> and C<sub>3</sub> plants suggest that the evolution of the C<sub>4</sub> phenotype required a large number and scale of changes (Hattersley 1984). Despite this apparent complexity, the C<sub>4</sub> trait evolved many times independently (Sage *et al.* 2011). Resolving this paradox requires the quantitative distinction of

changes that were involved in the evolutionary transition from C<sub>3</sub> to C<sub>4</sub>, from those that preceded or followed it.

In most C<sub>4</sub> plants, carbon fixation within leaf mesophyll tissue (M) is used to concentrate CO<sub>2</sub> and boost Rubisco activity within bundle sheath tissue (BS), whereas Rubisco in C<sub>3</sub> plants operates within the M where it depends on atmospheric CO<sub>2</sub> diffusion (Fig. 1; Brown 1975; Hattersley *et al.* 1977; Hatch 1987). Efficient C<sub>4</sub> leaves require large BS volumes to accommodate the necessary photosynthetic organelles, including chloroplasts containing abundant Rubisco, and a small distance between M and BS compartments to allow the rapid transfer of metabolites (Fig. 1; Hattersley & Watson 1975; Lundgren *et al.* 2014). These traits vary among C<sub>3</sub> plant lineages, and in grasses, C<sub>4</sub> photosynthesis evolved only within those groups with large fractions of BS (Christin *et al.* 2013; Lundgren *et al.* 2014). Comparisons of multiple C<sub>4</sub> lineages with their C<sub>3</sub> relatives indicate that the evolution of C<sub>4</sub> leaf anatomy involved ultrastructural rearrangements and further decreases to the relative volume of M compared to BS tissue (Hattersley 1984; Dengler *et al.* 1994; McKown & Dengler 2007; Christin *et al.* 2013). These properties can be achieved via a variety of leaf structural modifications, allowing C<sub>4</sub> anatomy to be realised differently each time it evolved, in some cases involving the use of different

<sup>1</sup>Department of Animal and Plant Sciences, University of Sheffield, Western Bank, Sheffield S10 2TN, UK

<sup>2</sup>Department of Ecology and Evolutionary Biology, University of Toronto, 25 Willcocks Street, Toronto, ON M5S 3B2, Canada

<sup>3</sup>Botany Department, Rhodes University, Grahamstown 6139, South Africa

<sup>4</sup>Comparative Plant and Fungal Biology, Royal Botanic Gardens, Kew, Richmond, Surrey TW9 3AB, UK

<sup>5</sup>Laboratoire Évolution & Diversité Biologique (EDB UMR5174), Université de Toulouse, CNRS, ENSFEA, UPS, IRD, 118 route de Narbonne, 31062, Toulouse, France

<sup>6</sup>Northern Territory Herbarium, Department of Environment and Natural Resources, PO Box 496, Palmerston, NT 0831, Australia

<sup>7</sup>National Herbarium and Botanic Garden, Harare, Zimbabwe

<sup>8</sup>Department of Primary Industry and Fisheries, Northern Territory Government, Darwin, NT 0801, Australia

<sup>†</sup>Present address: Lancaster Environment Centre, Lancaster University, Lancaster LA1 4YQ, UK

\*Correspondence: E-mail: c.p.osborne@sheffield.ac.uk

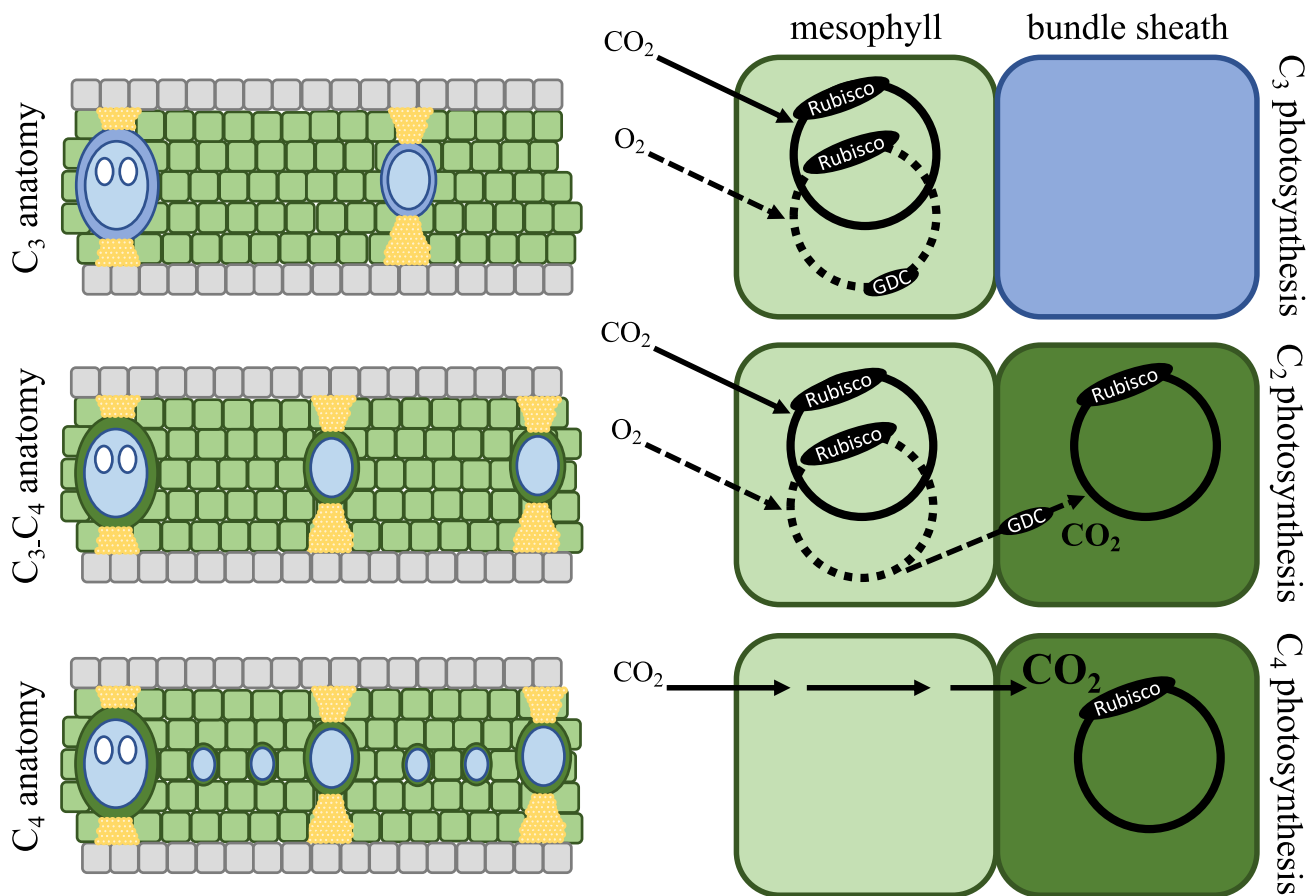


**Figure 1** Schematic of leaf anatomy and photosynthetic pathway in C<sub>3</sub>, C<sub>3</sub>-C<sub>4</sub> and C<sub>4</sub> grasses. In C<sub>3</sub> plants, CO<sub>2</sub> assimilation via the Calvin–Benson cycle (solid black circle) and CO<sub>2</sub> release via photorespiration (dashed black circle) both occur in mesophyll cells (light green). C<sub>3</sub> leaves consequently have larger areas of mesophyll tissue than bundle sheath tissue, where no photosynthetic activity occurs. C<sub>3</sub>-C<sub>4</sub> plants use an intermediate physiology called C<sub>2</sub> photosynthesis, where the Calvin-Benson cycle occurs in mesophyll cells, like in C<sub>3</sub> plants. However, because glycine decarboxylase (GDC) is specifically localised to bundle sheath cells in these plants, the photorespiratory cycle is split across these two cell types, creating a weak CO<sub>2</sub>-concentrating mechanism, where CO<sub>2</sub> is released in the bundle sheath and can be reassimilated via the Calvin cycle. C<sub>2</sub> photosynthesis, therefore, requires large areas of mesophyll for photosynthesis via an initial Calvin-Benson cycle, but also close contact between mesophyll and bundle sheath cells for the photorespiratory CO<sub>2</sub> pump. C<sub>4</sub> plants have a strong CO<sub>2</sub> concentrating mechanism whereby CO<sub>2</sub> is biochemically shuttled from the mesophyll into the bundle sheath. The high CO<sub>2</sub> concentration in the bundle sheath largely avoids oxygenation and thus, photorespiration. Photosynthesis via the C<sub>4</sub> cycle therefore requires large areas of bundle sheath tissue, but less mesophyll, which can be achieved via the insertion of minor veins. Dark blue, bundle sheath lacking chloroplasts; dark green, bundle sheaths with chloroplasts; light green, mesophyll cells; yellow, extraxylary fibres/bundle sheath extensions; grey, epidermal cells; light blue, veins; white, metaxylem.

tissue types for the C<sub>4</sub> BS function (Brown 1975; Soros & Dengler 2001; Christin *et al.* 2013; Freitag & Kadereit 2014; Lundgren *et al.* 2014). While the differences between a diverse range of C<sub>3</sub> and C<sub>4</sub> species are well known, the minimum set of leaf anatomical modifications required to carry out C<sub>4</sub> photosynthesis remains to be established.

The grass *Alloteropsis semialata* (R.Br.) Hitchc. provides an outstanding system to capture the early events during C<sub>4</sub> evolution because it includes genetically divergent C<sub>4</sub> individuals as well as a diversity of non-C<sub>4</sub> plants encompassing C<sub>3</sub> and C<sub>3</sub>-C<sub>4</sub> intermediate phenotypes (Ellis 1974; Lundgren *et al.* 2016), which emerged in the palaeotropics (Lundgren *et al.* 2015). The inner sheath (i.e., the mestome sheath), which is present in all C<sub>3</sub> grasses, has been co-opted for the C<sub>4</sub> BS function in *A. semialata*. Previous studies have compared leaf properties among C<sub>4</sub> and non-C<sub>4</sub> leaves of a few *A. semialata* accessions (Ellis 1974; Frean *et al.* 1983; Ueno & Sentoku 2006; Lundgren *et al.* 2016; Dunning *et al.* 2017), but a

broader sampling is required to establish which properties are unique to each photosynthetic type.

The primary focus of this study is to compare leaf anatomy in accessions spanning the diversity of each photosynthetic type to distinguish the structural diversifications that occurred before, during and after C<sub>4</sub> emergence in this species. We hypothesise that the properties that predate C<sub>4</sub> evolution will be shared by at least some of the non-C<sub>4</sub> individuals, while those that happened after C<sub>4</sub> evolution in a phase of subsequent adaptation will be restricted to a subset of the C<sub>4</sub> populations. Properties unique to, and common among all, C<sub>4</sub> accessions represent those that were involved in the initial transition to a C<sub>4</sub> physiology. We conducted a large scan of the diversity within the species using traits linked to the number and size of different cell types and used controlled growth experiments to verify that anatomical differences are not environmentally induced. This evaluation of the gross leaf morphology was accompanied by a focused study in some

individuals to identify ultrastructural changes that may also differ between C<sub>4</sub> and non-C<sub>4</sub> accessions. Overall, our work shows that a complex trait of large ecological significance can evolve via a few key developmental changes.

## MATERIALS AND METHODS

### Characterising photosynthetic types

Photosynthetic type was determined by a combination of stable isotope and CO<sub>2</sub> compensation point (CCP) data (Table S1; Data set S1), as previously described (Lundgren *et al.* 2016). The carbon isotope composition of plant tissues ( $\delta^{13}\text{C}$ ) distinguishes photosynthetic types (von Caemmerer *et al.* 2014), such that plants with  $\delta^{13}\text{C}$  values higher than  $-17\text{‰}$  were considered to have a fully functioning C<sub>4</sub> system, while those with values lower than this threshold were considered either C<sub>3</sub> or C<sub>3</sub>-C<sub>4</sub>. CCPs were used to distinguish C<sub>3</sub>-C<sub>4</sub> from C<sub>3</sub> plants and to support the  $\delta^{13}\text{C}$  results. The CCP indicates the CO<sub>2</sub> concentration within the leaf at which CO<sub>2</sub> assimilation via photosynthesis equals CO<sub>2</sub> loss via photorespiration and respiration. As less CO<sub>2</sub> is ultimately lost to photorespiration in C<sub>3</sub>-C<sub>4</sub> plants, they have very low CCPs compared to C<sub>3</sub> plants. Thus, non-C<sub>4</sub> plants with CCPs greater than or equal to 35  $\mu\text{mol mol}^{-1}$  were classified as C<sub>3</sub>, while those < 35  $\mu\text{mol mol}^{-1}$  were classified as C<sub>3</sub>-C<sub>4</sub>. CCPs were calculated on 27 living accessions (6 C<sub>3</sub>, 4 C<sub>3</sub>-C<sub>4</sub> and 17 C<sub>4</sub>), following published protocols (Bellasio *et al.* 2016a,b; Lundgren *et al.* 2016). Non-C<sub>4</sub> accessions for which live material was unavailable were assumed to have the same photosynthetic type as their closest relatives, as identified by phylogenetic relationships (Table S1).

### Leaf samples

Fifty *Alloteropsis semialata* (R.Br.) Hitchc. accessions distributed across the species' geographic range, including 17 C<sub>3</sub>, 6 C<sub>3</sub>-C<sub>4</sub> and 27 C<sub>4</sub>, were used to assess intraspecific anatomical variation. Leaf samples from 44 of the 50 accessions were collected from their original field site and preserved until embedding was possible. For the remaining six accessions, leaf samples were taken from plants grown under controlled environment conditions as in Lundgren *et al.* (2016). For all samples, leaf pieces 3–5 mm in length were embedded in methacrylate embedding resin (Technovit 7100, Heraeus Kulzer GmbH, Wehrheim, Germany), sectioned 6–8  $\mu\text{m}$  thick on a manual rotary microtome (Leica Biosystems, Newcastle, UK) and stained with Toluidine Blue O (Sigma-Aldrich, St. Louis, MO, USA). Stained leaf sections were imaged using microscopy imaging software with a camera mounted on a microscope (Cell A, Olympus DP71 and Olympus BX51, respectively; Olympus, Hamburg, Germany) and the images were stitched together using DoubleTake (v2.2.9, Echo One, Frederikssund, Denmark).

### Leaf anatomy measurements

Anatomical traits were measured using ImageJ (Fig. S1; Schneider *et al.* 2012) from the cross section of a single leaf

segment from the centre of the leaf blade, avoiding segments immediately adjacent to the midrib and lateral edges of the cross section. Vein orders were distinguished following Renvoize (1987). A single segment was defined as the leaf area falling between two secondary veins, which are large veins with metaxylem. Tertiary and minor veins (e.g. quaternary and quinary orders) lack metaxylem. In this species, the extraxylary fibres that flank both the adaxial and abaxial edges of tertiary veins distinguish them from higher order minor veins, which can be flanked by fibres on one side only (Fig. S1).

The cross-sectional area of the whole segment, combining M, BS, epidermis and bulliform cells, extraxylary fibres and BS extensions as well as any transverse veins or tear spaces was measured. For all accessions, the total BS (i.e. the inner sheath; the compartment used for the Calvin cycle in C<sub>4</sub> *A. semialata*), outer sheath and vein areas were measured separately for secondary, tertiary and any minor veins. The area of M tissue was calculated as the total area remaining after accounting for all other tissue types. In addition, the cross-sectional area of individual M and BS cells (hereafter 'size') was measured (Fig. S1). Although the depth of individual cells can vary, it is their cross-sectional areas, and not their three-dimensional volumes, that primarily influence the proportion of each tissue in the leaf.

### Linear discriminant analysis

We used a linear discriminant analysis (LDA) to explain the variation between photosynthetic types (i.e. the test maximises between-group variance while minimising within-group variance). We performed the LDA on the 50 accessions with leave-one-out cross-validation and then bootstrapping over 100 runs, using the MASS package in R (Venables & Ripley 2002). Prior probabilities were based on the relative sample size of the categorical variable (i.e. 0.34, 0.12 and 0.54 for C<sub>3</sub>, C<sub>3</sub>-C<sub>4</sub> and C<sub>4</sub> groups respectively). We chose predictor variables that were likely to influence the M : BS ratio, including the number of M cells between major veins, average size of individual M cells, number of minor veins per segment, leaf thickness and the average size of BS cells on tertiary veins.

To test the generality of our findings from *A. semialata*, we carried out an equivalent LDA for a larger sample of 157 grasses including one C<sub>3</sub> and one C<sub>4</sub> *A. semialata* and representing 17 independent C<sub>4</sub> lineages. Predictor variables in this analysis were based on the anatomical measurements of Christin *et al.* (2013) and chosen to best match the variables used in the *A. semialata* LDA described above, including the number of mesophyll cells between veins, mesophyll cell width, proportion of veins that are minor, leaf thickness, inner BS cell width and outer BS cell width. The species were grouped as C<sub>3</sub>, C<sub>4</sub> species using the inner BS and C<sub>4</sub> species using the outer BS.

### Vein order analysis

To determine whether the pattern of vein density observed in the main data set was maintained across a larger sample of *A. semialata*, we counted the total number of veins per

segment and the presence or absence of minor veins in 91 additional accessions consisting of herbarium specimens that had been rehydrated in distilled water overnight at 4°C prior to embedding, sectioning, staining and imaging as described above. Together with the 50 previous samples, this larger data set included a total of 72 C<sub>4</sub> (i.e.  $\delta^{13}\text{C} > -17\text{‰}$ ) and 69 non-C<sub>4</sub> (i.e.,  $\delta^{13}\text{C} < -17\text{‰}$ ) accessions distributed across the species' geographic range.

### Ultrastructure and immunohistochemistry

To investigate whether ultrastructural changes might differ between photosynthetic types within this species, we analysed the spatial distributions of organelles and enzymes in one population representing each of the C<sub>3</sub>, C<sub>3</sub>-C<sub>4</sub> and C<sub>4</sub> types. Recently expanded mature leaf tissue was prepared for transmission electron microscopy and processed for immunodetection of the large subunit of Rubisco (RBCL) and glycine decarboxylase H subunit (GLDH) as previously described (see Supporting Information Materials 1; Khoshravesh *et al.* 2017).

### Leaf anatomy in a common environment

To determine the degree to which the various leaf anatomical phenotypes arose from plastic development responses to their differing native growth environments, we compared field phenotypes to those obtained from live tillers of 17 *A. semialata* accessions (5 C<sub>3</sub>, 4 C<sub>3</sub>-C<sub>4</sub> and 8 C<sub>4</sub>) after growing for a minimum of 3 months in a common growth chamber, with conditions as described in Lundgren *et al.* 2016. The environmental conditions (Fick & Hijmans 2017) at the field collection sites are detailed in Table S2. On controlled environment samples, the number and order of veins, minimum number of M cells separating veins, area of inner BS cells, segment length and thickness, and IVD were determined on one segment per leaf.

### Plasticity for leaf anatomy in response to low CO<sub>2</sub>

To further test whether C<sub>4</sub>-compatible phenotypes could emerge from plastic responses to the environment, as previously suggested (Li *et al.* 2014), we carried out a CO<sub>2</sub> manipulation experiment designed to promote photorespiration. One C<sub>4</sub> (MDG, South Africa) and one C<sub>3</sub> (GMT, South Africa) plant were initially grown from seed in a controlled environment chamber set as described in Lundgren *et al.* 2016, but with 400  $\mu\text{mol mol}^{-1}$  CO<sub>2</sub> concentration. Both plants were split into five replicate cuttings and kept in the same growth chamber conditions to re-establish for four months. From each replicated clone, one fully expanded, mature leaf was sampled and fixed in 4 : 1 ethanol : acetic acid solution. The growth chamber was then set to 180  $\mu\text{mol mol}^{-1}$  CO<sub>2</sub> concentration for the next four months to promote photorespiration, while maintaining the other environmental conditions, and one new fully expanded leaf was again sampled and fixed. All leaf samples from the 400 (i.e. ambient) and 180 (i.e. low) CO<sub>2</sub> treatments were embedded, sectioned and imaged as described above. To determine whether the plants used different photosynthetic pathways in the two CO<sub>2</sub> growth

environments, we determined CCP and carboxylation efficiency, as described in Lundgren *et al.* (2016).

## RESULTS

### *Alloteropsis semialata* presents a continuum of leaf anatomy

The ratio of M to BS tissue, a trait known to differ among C<sub>3</sub> and C<sub>4</sub> species (Hattersley 1984), forms a continuum within *Alloteropsis semialata*, along which photosynthetic types are sorted (Fig. 2). Indeed, the smallest values are restricted to C<sub>4</sub> accessions and the largest are found in C<sub>3</sub> individuals. When considering the area in cross section between two secondary veins (i.e., a leaf segment from here onwards; Fig. S1), the M area is over 10 times larger than the BS area in C<sub>3</sub> accessions, but less than five times larger in C<sub>4</sub> accessions (Data set S1). As expected, C<sub>3</sub>-C<sub>4</sub> accessions are intermediate in their overall leaf anatomy, with 5–10 times more M than BS. These M : BS ranges are consistent with those measured in other C<sub>3</sub> and C<sub>4</sub> grasses (Christin *et al.* 2013).

### C<sub>3</sub>, C<sub>3</sub>-C<sub>4</sub> and C<sub>4</sub> *Alloteropsis semialata* have distinct leaf anatomy

Variation in M : BS ratios can arise via changes to several underlying traits (Lundgren *et al.* 2014). Our modelling shows that M area is the product of leaf thickness and interveinal distance (IVD; Table 1). The latter is predicted by the number and size of M cells between veins (Table 1). BS area is explained by the number of BS units (i.e. the number of veins per segment) and the size of BS cells (Table 1). When these

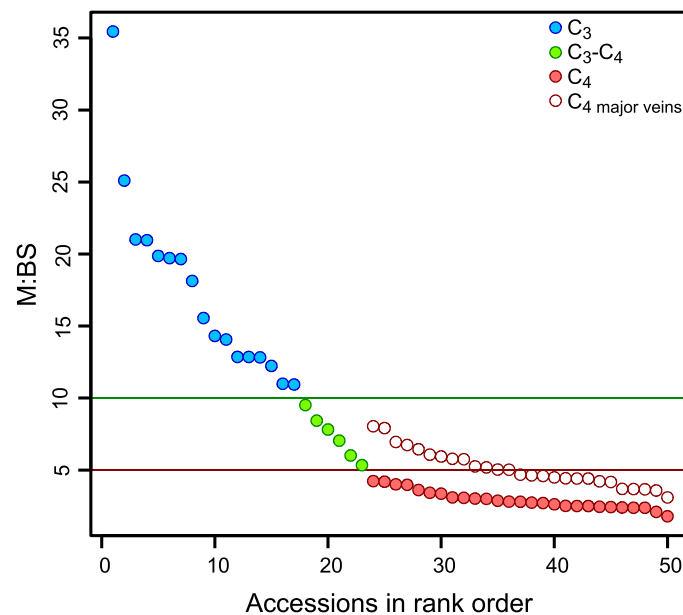


**Figure 2** Continuous variation in *Alloteropsis semialata* leaf anatomy, but distinct division among C<sub>3</sub>, C<sub>3</sub>-C<sub>4</sub> and C<sub>4</sub> types. Ratios of mesophyll (M) to bundle sheath (BS) area of individual accessions of C<sub>3</sub> (blue circles), C<sub>3</sub>-C<sub>4</sub> (green circles) and C<sub>4</sub> (solid red circles) plants, ranked by M:BS value.  $n = 50$ . Lines delineating M:BS ratios that distinguish C<sub>3</sub> from C<sub>3</sub>-C<sub>4</sub> (green) and C<sub>3</sub>-C<sub>4</sub> from C<sub>4</sub> (red) are shown. For C<sub>4</sub> individuals, M:BS ratios are also calculated in the absence of minor veins (open red circles).



**Table 1** Results of linear regression analyses on leaf components underlying M : BS ratios in *Alloteropsis semialata*

	<i>F</i>	df	Adj <i>R</i> <sup>2</sup>	<i>P</i>	<i>t</i>	<i>P</i>
Total M area/segment (μm <sup>2</sup> )	59.35	2, 47	0.704	1.38 × 10 <sup>-13</sup>	3.98	0.00024
Leaf thickness (μm)					10.58	5.07 × 10 <sup>-14</sup>
Interveinal distance* (μm)						
Interveinal distance (μm)	343.4	2, 47	0.933	< 2.2 × 10 <sup>-16</sup>		
Number M cells between veins <sup>†</sup>					25.48	< 2 × 10 <sup>-16</sup>
M cell size (μm <sup>2</sup> )					6.97	9.22 × 10 <sup>-9</sup>
Total BS area/segment (μm <sup>2</sup> )	124.8	2, 47	0.835	< 2.2 × 10 <sup>-16</sup>		
BS cell size <sup>‡</sup> (μm <sup>2</sup> )					9.52	1.54 × 10 <sup>-12</sup>
Vein density (veins/segment)					4.23	0.00011

\*Average distance between the center points of all veins.

<sup>†</sup>Number of mesophyll (M) cells between all veins.

<sup>‡</sup>Cross-sectional area of inner bundle sheath (BS) cells on tertiary order veins.

potential explanatory traits are incorporated within an LDA, all variance between the three photosynthetic types is captured (Fig. 3a). In a bootstrapped sample, the mean overall predictive accuracy is 0.986, which is statistically indistinguishable from 1.0 (95% CI = 0.966–1.000). The mean predictive accuracy for C<sub>4</sub> (0.999, 95% CI = 0.995–1.000), C<sub>3</sub> (0.976, 95% CI = 0.918–1.000) and C<sub>3</sub>-C<sub>4</sub> (0.926, 95% CI = 0.805–1.000) accessions is also statistically indistinguishable from 1.0. The analysis, therefore, confirms that leaf anatomy varies among photosynthetic types in a statistically predictable manner.

The first axis of the LDA explains 97.37% of the variance between photosynthetic types and clearly distinguishes C<sub>4</sub> from non-C<sub>4</sub> accessions (Fig. 3a). This axis is most strongly associated with the number of minor veins per segment, which were absent from all non-C<sub>4</sub> accessions in this analysis (Table 2). The second axis explains 2.63% of the variance between groups, clearly distinguishes C<sub>3</sub> from C<sub>3</sub>-C<sub>4</sub> plants, and is most strongly associated with the number of M cells between major veins (i.e. secondary and tertiary order veins) and the number of minor veins (Fig. 3a; Table 2). Since minor veins are restricted to C<sub>4</sub> individuals, their contribution to LD2 is linked to diversity within the C<sub>4</sub> group. These results indicate that most of the variance in the data set stems from the contrast between C<sub>4</sub> and non-C<sub>4</sub> individuals and is driven entirely by a single underlying trait, the presence of minor veins. The phenotypic distance between C<sub>3</sub> and C<sub>3</sub>-C<sub>4</sub> individuals is very small, being explained by the number of M cells between major veins. Conversely, leaf thickness and the cross-sectional areas of individual BS and M cells poorly distinguish photosynthetic types in this species.

The first two axes of an LDA of anatomical traits on the larger species data set explain 89.62% and 10.38% of the variation respectively. The first axis clearly distinguishes C<sub>4</sub> species that use the inner bundle sheath from C<sub>4</sub> species using the outer sheath and the C<sub>3</sub> species (Fig. 3b) and is mostly associated with the proportion of minor veins, while the remaining anatomical traits are weakly correlated with both axes (Table 2).

#### Differences between C<sub>4</sub> and non-C<sub>4</sub> phenotypes arise from the development of minor veins

In *A. semialata*, the presence of minor veins is the only variable consistently distinguishing C<sub>4</sub> and non-C<sub>4</sub> accessions. When the M : BS ratio is calculated in the absence of minor

veins, the clear distinction between C<sub>3</sub>-C<sub>4</sub> and C<sub>4</sub> accessions disappears, with nearly half the C<sub>4</sub> accessions overlapping with C<sub>3</sub>-C<sub>4</sub> plants (Fig. 2). This shows that the development of minor veins in C<sub>4</sub> accessions reduces the M : BS ratio by increasing BS area and displacing M area. To confirm the restriction of minor veins to C<sub>4</sub> individuals, we screened vein architecture in a larger data set of *A. semialata* (Fig. 4a,b; Data set S2). Minor veins were present in all C<sub>4</sub> accessions and absent in all but five non-C<sub>4</sub> accessions. Four of these had only occasional and irregularly spaced minor veins, while the final accession is an individual originating from a natural cross between C<sub>3</sub>-C<sub>4</sub> and C<sub>4</sub> individuals (Olofsson *et al.* 2016). Our data therefore show that the presence of frequent and regularly spaced minor veins is universally and uniquely associated with the C<sub>4</sub> genomic background, captures nearly all of the anatomical variation between C<sub>4</sub> and non-C<sub>4</sub> phenotypes and explains overall differences in relative M and BS areas.

The proliferation of minor veins explains a number of patterns associated with C<sub>4</sub> anatomy. As expected, the number of M cells between consecutive veins differs among photosynthetic types, being the smallest in C<sub>4</sub> accessions (1–3), compared to C<sub>3</sub>-C<sub>4</sub> (3–6) and C<sub>3</sub> (5–11) plants (Fig. S2). However, the number of M cells between major veins overlaps between the C<sub>4</sub> and non-C<sub>4</sub> groups (Fig. 4c), which indicates that the reduced distance between any pair of M and BS cells in C<sub>4</sub> accessions is caused by the differentiation of ground meristem cells into minor veins rather than a reduced proliferation of M cells. The high vein density of C<sub>4</sub> plants following the development of minor veins is accompanied by more than a twofold increase in extraxylary fibres (i.e. tissue area per segment length) than is found in non-C<sub>4</sub> accessions (Fig. S3). As the area of extraxylary fibres per vein does not differ between the photosynthetic types (Fig. S3), the increased fibre area in C<sub>4</sub> plants derives entirely from their greater vein density.

#### Other anatomical changes happened before or after the transition from C<sub>3</sub>-C<sub>4</sub> to C<sub>4</sub> physiology

The development of minor veins explains the overall anatomical difference between C<sub>4</sub> and non-C<sub>4</sub> accessions and is therefore linked to the emergence of a fully functioning C<sub>4</sub> physiology from a C<sub>3</sub>-C<sub>4</sub> intermediate state. Evolutionary changes that happened once this C<sub>4</sub> physiology was in place would be restricted to some, but not all, C<sub>4</sub> individuals. In

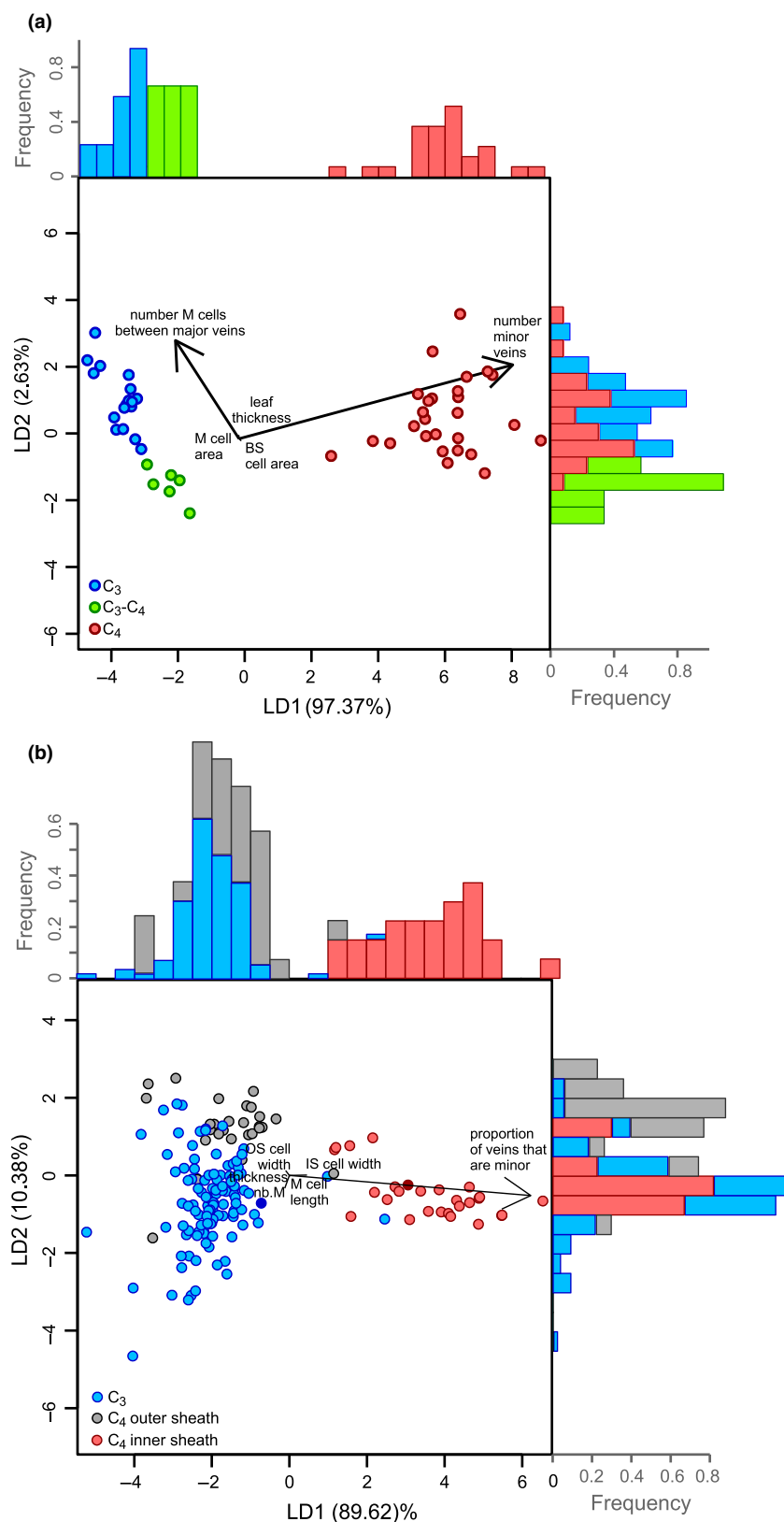


**Figure 3** Linear discriminant analysis of leaf anatomical traits. The first (LD1) and second (LD2) dimensions of the LDA are plotted against each other with histograms of each dimension shown on the opposing axis for (a) the LDA on  $C_3$ ,  $C_3$ - $C_4$  and  $C_4$  *Alloteropsis semialata* accessions and (b) the LDA on 157  $C_3$ ,  $C_4$  inner sheath and  $C_4$  outer sheath grass species. In addition, one  $C_3$  and one  $C_4$  *A. semialata* accession were included in this larger LDA and are denoted by solid blue and red circles respectively. Loading plots are overlaid via black arrows. M, mesophyll; IS, inner sheath; OS, outer sheath; nb.M, number of mesophyll cells between veins.

**Table 2** Coefficients of linear discriminants in a linear discriminant analysis on (top) five leaf anatomical traits expected to drive overall mesophyll to bundle sheath area ratios in *Alloteropsis semialata* and on (bottom) six leaf anatomical traits in 157 grass species, grouped as C<sub>3</sub> species, C<sub>4</sub> species using the inner sheath and C<sub>4</sub> species using the outer sheath

LDA on *Alloteropsis semialata* accessions

Trait	LD1	LD2
Number of minor veins per segment	1.3591	0.3663
Number of mesophyll cells between major veins	-0.315	0.4881
Average area inner bundle sheath cell on tertiary veins ( $\mu\text{m}^2$ )	0.0123	-0.0104
Average area mesophyll cell ( $\mu\text{m}^2$ )	-0.0012	-7.82E-05
Leaf thickness ( $\mu\text{m}$ )	-5.52E-04	0.0189

LDA on 157 grass species + 1 C<sub>3</sub> and 1 C<sub>4</sub> *Alloteropsis semialata* accession

Trait	LD1	LD2
Proportion of veins that are minor	4.145779	-0.34605
Outer bundle sheath (BS) cell width ( $\mu\text{m}$ )	-0.06433	0.080823
Inner BS cell width ( $\mu\text{m}$ )	0.301257	0.004749
Leaf thickness ( $\mu\text{m}$ )	-0.0083	-0.00729
Mesophyll cell width ( $\mu\text{m}$ )	0.01989	-0.01048
Number of mesophyll cells between veins	-0.08007	-0.22237

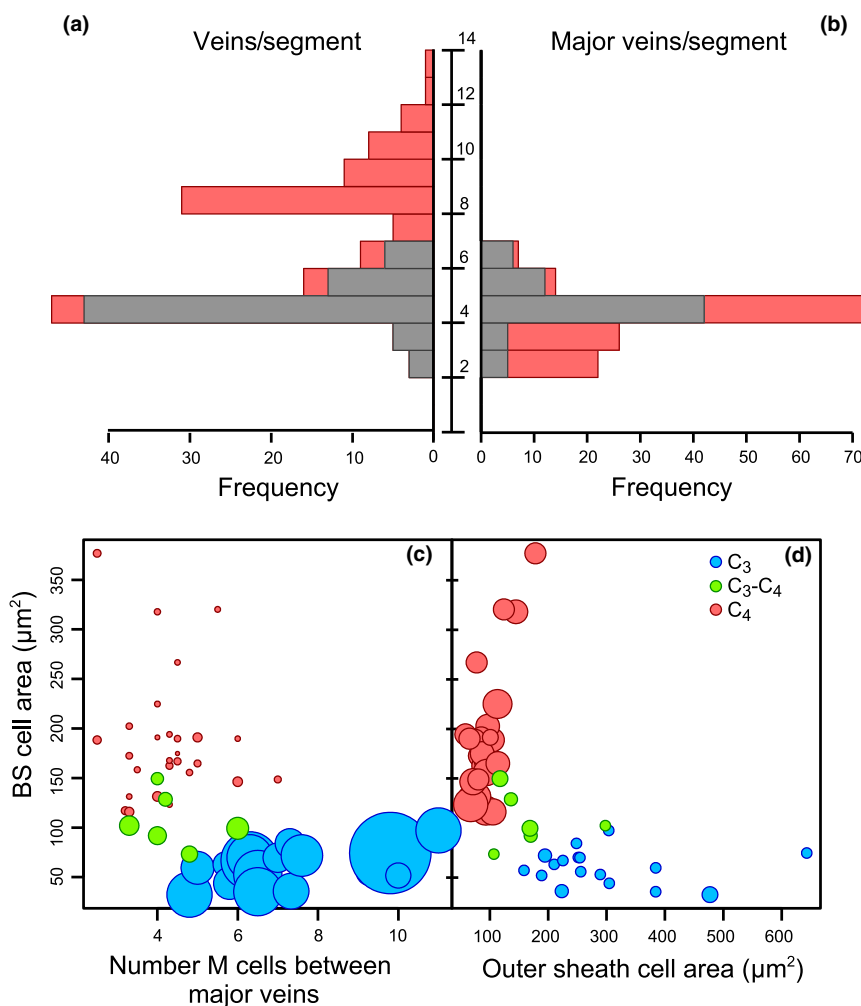


**Figure 4** Diversity of intraspecific anatomical components. Histograms of (a) vein density (i.e., the total number of veins per segment) and (b) the number of major veins per segment in C<sub>4</sub> (red;  $n = 72$ ) and non-C<sub>4</sub> (grey;  $n = 69$ ) accessions. Scatter plots show (c) the average number of mesophyll (M) cells between major veins vs. the average area of individual bundle sheath (BS) cells, with dot size proportional to the M:BS ratio, and (d) BS cell area vs. outer sheath cell area, with dot size proportional to the number of veins per segment. Colours indicate photosynthetic type with C<sub>3</sub> (blue;  $n = 17$ ), C<sub>3</sub>-C<sub>4</sub> (green;  $n = 6$ ) and C<sub>4</sub> (red;  $n = 27$ ).

our data set, such changes include further reductions to the M : BS ratio, potentially achieved via contractions to M airspace (Byott 1976) or increases in BS cell size. Indeed, although BS cell sizes of different photosynthetic types overlap, large increases to BS cell size characterise some African C<sub>4</sub> accessions (Figs S4 and S5). The BS cell enlargement was therefore involved in the adaptation of C<sub>4</sub> physiology after it had emerged, possibly to accommodate more or larger organelles for a more efficient C<sub>4</sub> cycle, rather than being involved in its origin. Occasional hybridisation between C<sub>4</sub> and non-C<sub>4</sub> individuals could affect the distribution of trait values; however, non-C<sub>4</sub> *A. semialata* individuals are restricted to Africa, so that hybridisation outside of Africa is unlikely. Yet, Asia and Australian accessions exhibit some of the smallest BS cells among C<sub>4</sub> accessions (Fig. S5).

Some characters observed in C<sub>4</sub> accessions are also present in C<sub>3</sub>-C<sub>4</sub> individuals, but not C<sub>3</sub> ones, indicating that they are not associated with the transition to fully functional C<sub>4</sub> physiology, but might have facilitated it. These include a small increase in BS cell sizes in C<sub>3</sub>-C<sub>4</sub> compared with C<sub>3</sub> plants and a decrease in outer sheath cell size, with C<sub>3</sub>-C<sub>4</sub> accessions bridging the anatomical gap between C<sub>3</sub> and C<sub>4</sub> outer sheath cell sizes (Fig. 4c,d). This reduced outer sheath in C<sub>3</sub>-C<sub>4</sub> and C<sub>4</sub> *A. semialata* likely facilitates metabolite exchanges between M and BS cells.

#### Differences between C<sub>4</sub> and non-C<sub>4</sub> leaves are not environmentally induced

*Alloteropsis semialata* plants grow naturally in diverse environments, depending on their photosynthetic background and evolutionary history (Lundgren *et al.* 2015). To verify that the differences we observe among photosynthetic types are not induced by environmental variations, we compared the leaves of field-collected plants after transplanting and growing them in a common controlled environment growth chamber for at least 3 months (Data set S3; Fig. S6). Compared to field conditions, C<sub>3</sub> accessions produced more M cells between veins ( $P = 0.044$ ) in the common environment. Moreover, C<sub>3</sub>-C<sub>4</sub> plants produced thicker leaves ( $P = 0.040$ ), such that leaf thickness of the three photosynthetic types converged in the common environment, which is likely a result of the non-limiting light, nutrients and water available in these conditions. However, the other traits were not influenced by growth conditions and leaf anatomy of the three photosynthetic types remained distinct when grown in the common environment.

We further verified that historical changes in atmospheric composition did not influence the leaf phenotype by comparing C<sub>3</sub> and C<sub>4</sub> *A. semialata* under current ambient (400 ppm) and the Pleistocene minimum (180 ppm) CO<sub>2</sub> concentrations. Plants grown under the low CO<sub>2</sub> concentration experience elevated photorespiration rates, which might have induced a more C<sub>4</sub>-like anatomy. However, we found that plants did not shift photosynthetic state under the differing CO<sub>2</sub> conditions (i.e. mean CCPs in ambient/low CO<sub>2</sub> for C<sub>3</sub> = 49.8/53.1 and C<sub>4</sub> = 4.6/8.1  $\mu\text{mol mol}^{-1}$ ; Data set S4). Both C<sub>3</sub> and C<sub>4</sub> plants produced thinner leaves in the low CO<sub>2</sub> environment ( $P = 0.0049$  C<sub>3</sub>/0.0065 C<sub>4</sub>), and C<sub>4</sub> plants developed smaller BS cells ( $P = 0.011$ ; Fig. S6), probably because the lower

carbon supply restricted development (Ripley *et al.* 2013). Importantly, the C<sub>3</sub> plants did not produce more veins (or any minor veins), larger BS cells or fewer M cells between veins when grown under this high photorespiration condition. These results show that, even when photorespiration is high, a C<sub>4</sub>-like phenotype is not plastically induced in C<sub>3</sub> *A. semialata*.

#### DISCUSSION

Photosynthetic types form a continuum, along which multiple biochemical, anatomical and ultrastructural alterations increase the proportion of CO<sub>2</sub> fixed via the C<sub>4</sub> cycle. The emerging model of C<sub>4</sub> evolution involves gradual and overlapping phenotypic changes (Heckmann *et al.* 2013; Sage *et al.* 2014; Bräutigam & Gowik 2016; Schlüter & Weber 2016; Dunning *et al.* 2017), with traits acquired in differing orders among C<sub>4</sub> lineages (Williams *et al.* 2013). Different traits may be involved in the initial transition to a C<sub>4</sub> phenotype and the subsequent adaptation and diversification of that phenotype (Christin & Osborne 2014; Watcharamongkol *et al.* 2018). Within the grass *Alloteropsis semialata*, we have shown that the only gross leaf property distinguishing all C<sub>4</sub> from all non-C<sub>4</sub> phenotypes is the development of frequent minor veins. The presence of these minor veins has multiple consequences, including an overall increase in vein density, enlargement of the total volumes of BS tissue and a displacement of M tissue. These anatomical changes combine to facilitate C<sub>4</sub> cycle activity, as demonstrated by a strong correlation between leaf vein frequency and carbon isotope composition observed for this species (Lundgren *et al.* 2016). Our analyses of leaf ultrastructure indicate that the evolution of C<sub>4</sub> photosynthesis in *A. semialata* may have involved additional changes in organelle distribution among cell types (Supporting Information Materials 1; Figs S7–S9), although the small sample of populations prevents us from differentiating ultrastructural changes linked to the transition to C<sub>4</sub> from those that happened later.

The change in venation inferred during the evolution of C<sub>4</sub> photosynthesis in *A. semialata* may have a number of physiological and ecological consequences. First, the increase in vein frequency is accompanied by an enhancement of unpigmented extraxylary fibres, which improves light transmission to the BS, and thus ATP production in these cells, facilitating photosynthetic carbon reduction (Bellasio & Lundgren 2016). Enhanced fibre density may also increase leaf toughness, reduce digestibility and consequently deter herbivores (Caswell *et al.* 1973; Wilson *et al.* 1983). Secondly, the insertion of additional veins may influence leaf hydraulics. Model simulations for other plant species demonstrate that an increase in minor vein density can lead to greater leaf hydraulic conductance (McKown *et al.* 2010). However, empirical studies show that this is unlikely to improve drought tolerance, since the decline in hydraulic conductance during drought arises primarily outside veins (Scoffoni & Sack 2017; Scoffoni *et al.* 2017a), while embolisms arise first in the midrib, not minor veins (Scoffoni *et al.* 2017b).

Our results complement those from previous comparisons among species, which show that an additional order of minor veins develops during the evolutionary transition from non-C<sub>4</sub>



to C<sub>4</sub> forms of *Flaveria* (McKown & Dengler 2009), while BS cell size is large in both C<sub>3</sub> and C<sub>4</sub> *Flaveria* species (Kümpers *et al.* 2017). Our further analysis of leaf gross anatomy across multiple grass species shows that the insertion of additional minor veins is a frequent developmental mechanism for decreasing the M : BS ratio in those C<sub>4</sub> grasses that primarily localise Rubisco within the mestome sheath. The insertion of minor veins could occur via relatively few developmental changes, likely underpinned by changes to auxin, brassinosteroids, SHORTROOT/SCARECROW and/or INDETERMINATE DOMAIN transcription factors (Kumar & Kellogg 2018; Sedelnikova *et al.* 2018). In grasses, vein orders develop sequentially as leaves grow wider, such that minor veins are initiated considerably later than other vein orders, usually once the leaf ceases to widen (Nelson & Langdale 1989; Sedelnikova *et al.* 2018). Thus, the development of functional minor veins likely arises via the heterochronic regulation of the existing machinery for vein formation, sustaining vein differentiation beyond that of non-C<sub>4</sub> plants (Nelson 2011; Sedelnikova *et al.* 2018), probably through the prolonged production of auxin during later phases of leaf elongation (Scarpella *et al.* 2010). Alternatively, minor veins may also result from a heterotopic specialisation of auxin maxima that permits them to form closer together (Kumar & Kellogg 2018).

The possibility that a transition from non-C<sub>4</sub> to C<sub>4</sub> states can be caused by a single developmental alteration is a plausible explanation for the recurrent origins of C<sub>4</sub> leaf anatomy and helps to resolve the paradox of how this complex trait emerged so many times. We also show that organelle number and size differ among photosynthetic types of *A. semialata*, but, here too, recent work indicates that one gene can control multiple ultrastructural modifications (Wang *et al.* 2017). Finally, transcriptome comparisons show that few genes encoding enzymes are upregulated during the transition from non-C<sub>4</sub> to C<sub>4</sub> in *A. semialata* (Dunning *et al.* 2017). We therefore conclude that the overall transition from a non-C<sub>4</sub> state to the form of C<sub>4</sub> photosynthesis observed in *A. semialata* involved relatively few genetic mutations.

The limited number of changes involved in the emergence of C<sub>4</sub> anatomy in *A. semialata* is partially explained by the presence of relatively enlarged BS in the C<sub>3</sub>-C<sub>4</sub> accessions, while C<sub>3</sub> *A. semialata* BS size is similar to C<sub>3</sub> species from other grass lineages (Lundgren *et al.* 2014, 2016; Dunning *et al.* 2017). C<sub>3</sub>-C<sub>4</sub> *A. semialata* are also characterised by fewer M cells compared to C<sub>3</sub> accessions and higher BS organelle abundance (Figs 3a, 4c and S7–S9). These properties that had been selected for the C<sub>3</sub>-C<sub>4</sub> physiology eased the subsequent transition to a full C<sub>4</sub> state, but it is important to note that the physiology and anatomy of C<sub>3</sub>-C<sub>4</sub> *A. semialata* are typical for C<sub>3</sub>-C<sub>4</sub> plants in general (Lundgren *et al.* 2016), and their anatomical characteristics can be found among C<sub>3</sub> grasses (Hattersley 1984; Christin *et al.* 2013; Lundgren *et al.* 2014). The background against which C<sub>4</sub> anatomy evolved in *A. semialata* is therefore not exceptional.

Our conclusion that C<sub>4</sub> leaf anatomy can arise from one key developmental modification is apparently incompatible with the great anatomical specialisation of other C<sub>4</sub> lineages as well as the large phenotypic gaps separating them from their closest C<sub>3</sub> relatives (Dengler *et al.* 1994; Christin *et al.*

2013). However, most C<sub>3</sub> and C<sub>4</sub> sister lineages are separated by long periods of evolution, and comparing these groups therefore captures all of the changes that happened after the origin of C<sub>4</sub> photosynthesis to improve the efficiency of C<sub>4</sub> physiology and adapt it to various organismal and ecological contexts (Christin & Osborne 2014). Indeed, photosynthetic efficiency may be significantly lower in C<sub>4</sub> *A. semialata* than in species from some older C<sub>4</sub> lineages (Lundgren *et al.* 2016; Bräutigam *et al.* 2018). This suggests that C<sub>4</sub> photosynthesis in *A. semialata* may represent a rudimentary version of the physiological trait (Ueno & Sentoku 2006). The biochemical characteristics of the C<sub>4</sub> cycle in *A. semialata* may be one reason for this (Bräutigam *et al.* 2018), and the presence of Rubisco protein in M could be another (Ueno & Sentoku 2006). Anatomical diversity may also explain some of the variation in physiological efficiency among *A. semialata* populations (Lundgren *et al.* 2016). Indeed, in *A. semialata*, enlargements of the BS cells beyond those seen in non-C<sub>4</sub> individuals are restricted to a subset of C<sub>4</sub> populations (Fig. 2) and thus happened after the emergence of C<sub>4</sub> physiology. Over time, accumulated modifications will move C<sub>4</sub> leaf anatomy far beyond that realised via a single developmental change. However, the fact that an initial C<sub>4</sub> phenotype and the associated physiology can be accessed via a single modification likely placed multiple groups on a selective highway to highly specialised and successful variants of the C<sub>4</sub> syndrome.

#### ACKNOWLEDGEMENTS

This work was funded by a University of Sheffield Prize Scholarship to MRL, an ERC grant (grant number ERC-2014-STG-638333) and a Royal Society Research Grant (grant number RG130448). LTD and JKO are supported by a NERC grant (grant number NE/M00208X/1) and PAC is supported by a Royal Society University Research Fellowship (grant number URF120119). JWB was supported by 301 and Think Ahead Sheffield Undergraduate Research Experience grants to MRL. The work on ultrastructure was supported by a Natural Sciences and Engineering Research Council of Canada grant (no 2015-04878) to TLS. The authors thank Peter Westhoff, Stefanie Schulze and Udo Gowik for use of their GLDH antibody, Susanne von Caemmerer for advice about outer bundle sheath cell resistance, Paul Hattersley for leaf samples and <sup>13</sup>C isotope data, John Thompson for field assistance and sample collection, Emma Jardine for discussion of linear discriminant analysis, Heather Walker for mass spectrometry assistance, Gareth Fraser for the use of his vibratome and Emanuela Samaritani for histology assistance. Herbarium leaf samples were obtained from the Herbarium at the Royal Botanic Garden Kew, the National Herbarium of South Africa in Pretoria, National Museums of Kenya in Nairobi and the National Botanic Garden of Belgium, Brussels, with the assistance of Martin Xanthos, Lyn Fish, Caroline Mashau and Itambo Malombe.

#### AUTHORSHIP

MRL, PAC and CPO designed the study. MRL produced and analysed the data, with the help of LTD, JJMV and JWB. TS

and RK performed the immunolocalisations and TEM imaging. SS assisted with immunolocalisation sample preparation. MS assisted with tissue fixation. MRL, LTD, JKO, BR, MSV, GB, CA, NC, AM, MB, CML, PAC and CPO contributed plant material. MRL, PAC and CPO interpreted the results and wrote the paper, with the help of all the authors.

#### DATA ACCESSIBILITY STATEMENT

Data available from the Dryad Digital Repository: <https://doi.org/10.5061/dryad.q7r61k7>

#### REFERENCES

- Bellasio, C. & Lundgren, M.R. (2016). Anatomical constraints to C<sub>4</sub> evolution: light harvesting capacity in the bundle sheath. *New Phytol.*, 212, 485–496.
- Bellasio, C., Beerling, D.J. & Griffiths, H. (2016a). An Excel tool for deriving key photosynthetic parameters from combined gas exchange and chlorophyll fluorescence: theory and practice. *Plant, Cell Environ.*, 39, 1180–1197.
- Bellasio, C., Beerling, D.J. & Griffiths, H. (2016b). Deriving C<sub>4</sub> photosynthetic parameters from combined gas exchange and chlorophyll fluorescence using an Excel tool: theory and practice. *Plant, Cell Environ.*, 39, 1164–1179.
- Bräutigam, A. & Gowik, U. (2016). Photorespiration connects C<sub>3</sub> and C<sub>4</sub> photosynthesis. *J. Exp. Bot.*, 67, 2953–2962.
- Bräutigam, A., Schluter, U., Lundgren, M.R., Flachbart, S., Ebenhoh, O., Schonknecht, G. *et al.* (2018). Biochemical mechanisms driving rapid fluxes in C<sub>4</sub> photosynthesis. *bioRxiv*, 387431.
- Brown, W.V. (1975). Variations in anatomy, associations, and origins of Kranz tissue. *Am. J. Bot.*, 62, 395–402.
- Byott, G.S. (1976). Leaf air space systems in C<sub>3</sub> and C<sub>4</sub> species. *New Phytol.*, 76, 295–299.
- von Caemmerer, S., Ghannoum, O., Pengelly, J.J. & Cousins, A.B. (2014). Carbon isotope discrimination as a tool to explore C<sub>4</sub> photosynthesis. *J. Exp. Bot.*, 65, 3459–3470.
- Caswell, H., Reed, F., Stephenson, S.N. & Werner, P.A. (1973). Photosynthetic pathways and selective herbivory: a hypothesis. *Am. Nat.*, 107, 465–480.
- Chollet, R. & Ogren, W.L. (1975). Regulation of photorespiration in C<sub>3</sub> and C<sub>4</sub> species. *Bot. Rev.*, 41, 137–179.
- Christin, P.A. & Osborne, C.P. (2014). The evolutionary ecology of C<sub>4</sub> plants. *New Phytol.*, 204, 765–781.
- Christin, P.A., Osborne, C.P., Chatelet, D.S., Columbus, J.T., Besnard, G., Hodkinson, T.R. *et al.* (2013). Anatomical enablers and the evolution of C<sub>4</sub> photosynthesis in grasses. *Proc. Natl Acad. Sci.*, 110, 1381–1386.
- Dengler, N.G., Dengler, R.E., Donnelly, P.M. & Hattersley, P.W. (1994). Quantitative leaf anatomy of C<sub>3</sub> and C<sub>4</sub> grasses (Poaceae): bundle sheath and mesophyll surface area relationships. *Ann. Bot.*, 73, 241–255.
- Downton, W.J.S. & Tregunna, E.B. (1968). Carbon dioxide compensation-its relation to photosynthetic carboxylation reactions, systematics of the Gramineae, and leaf anatomy. *Can. J. Bot.*, 46, 207–215.
- Dunning, L.T., Lundgren, M.R., Moreno-Villena, J.J., Namaganda, M., Edwards, E.J., Nosil, P. *et al.* (2017). Introgression and repeated co-option facilitated the recurrent emergence of C<sub>4</sub> photosynthesis among close relatives. *Evolution*, 71, 1541–1555.
- Ehleringer, J.R., Sage, R.F., Flanagan, L.B. & Pearcy, R.W. (1991). Climate change and the evolution of C<sub>4</sub> photosynthesis. *Trends Ecol. Evol.*, 6, 95–99.
- Ellis, R.P. (1974). The significance of the occurrence of both Kranz and non-Kranz leaf anatomy in the grass species *Alloteropsis semialata*. *S. Afr. J. Sci.*, 70, 169–173.
- Fick, S.E. & Hijmans, R.J. (2017). Worldclim 2: new 1-km spatial resolution climate surfaces for global land areas. *Int. J. Climatol.*, 37, 4302–4315.
- Frean, M.L., Ariovich, D. & Cresswell, C.F. (1983). C<sub>3</sub> and C<sub>4</sub> Photosynthetic and anatomical forms of *Alloteropsis semialata* (R. Br.) Hitchcock: 2. A comparative investigation of leaf ultrastructure and distribution of chlorenchyma in the two forms. *Ann. Bot.*, 51, 811–821.
- Freitag, H. & Kadereit, G. (2014). C<sub>3</sub> and C<sub>4</sub> leaf anatomy types in Camphorosmeae (Camphorosmoideae, Chenopodiaceae). *Plant Syst. Evol.*, 300, 665–687.
- Hatch, M.D. (1976). Photosynthesis: the path of carbon. In: *Plant Biochemistry* (eds Bonner, J., Varner, J.). Academic Press, New York, USA, pp. 797–844.
- Hatch, M.D. (1987). C<sub>4</sub> photosynthesis: a unique blend of modified biochemistry, anatomy and ultrastructure. *Biochim. Biophys. Acta*, 895, 81–106.
- Hattersley, P.W. (1984). Characterization of C<sub>4</sub> type leaf anatomy in grasses (Poaceae). M:BS area ratios. *Ann. Bot.*, 53, 163–180.
- Hattersley, P.W. & Watson, L. (1975). Anatomical parameters for predicting photosynthetic pathways of grass leaves: the 'maximum lateral cell count' and the 'maximum cells distant count'. *Phytomorphology*, 25, 325–333.
- Hattersley, P.W., Watson, L. & Osmond, C.B. (1977). In situ immunofluorescent labelling of ribulose-1, 5-bisphosphate carboxylase in leaves of C<sub>3</sub> and C<sub>4</sub> plants. *Aust. J. Plant Physiol.*, 4, 523–539.
- Heckmann, D., Schulze, S., Denton, A., Gowik, U., Westhoff, P., Weber, A.P.M. *et al.* (2013). Predicting C<sub>4</sub> photosynthesis evolution: modular, individually adaptive steps on a Mount Fuji fitness landscape. *Cell*, 153, 1579–1588.
- Khoshraveh, R., Lundgaard-Nielsen, V., Sultmanis, S. & Sage, T.L. (2017). *Light Microscopy, Transmission Electron Microscopy, and Immunohistochemistry Protocols for Studying Photorespiration*. Photorespiration. Humana Press, New York, USA, pp. 243–270.
- Kumar, D. & Kellogg, E.A. (2018). Getting closer: vein density in C<sub>4</sub> leaves. *New Phytol.* <https://doi.org/10.1111/nph.15491>.
- Kümpers, M.C., Burgess, S.J., Reyna-Llorens, I., Smith-Unna, R., Bournnell, R. & Hibberd, J.M. (2017). Shared characteristics underpinning C<sub>4</sub> leaf maturation derived from analysis of multiple C<sub>3</sub> and C<sub>4</sub> species of *Flaveria*. *J. Exp. Bot.*, 68, 177–189.
- Li, Y., Xu, J., Haq, N.U., Zhang, H. & Zhu, X.G. (2014). Was low CO<sub>2</sub> a driving force of C<sub>4</sub> evolution: *Arabidopsis* responses to long-term low CO<sub>2</sub> stress. *J. Exp. Bot.*, 65, 3657–3667.
- Lundgren, M.R., Osborne, C.P. & Christin, P.A. (2014). Deconstructing Kranz anatomy to understand C<sub>4</sub> evolution. *J. Exp. Bot.*, 65, 3357–3369.
- Lundgren, M.R., Besnard, G., Ripley, B.S., Lehmann, C.E.R., Chatelet, D.S., Kynast, R.G. *et al.* (2015). Photosynthetic innovation broadens the niche within a single species. *Ecol. Lett.*, 18, 1021–1029.
- Lundgren, M.R., Christin, P.A., Gonzalez Escobar, E., Ripley, B.S., Besnard, G., Long, C.M. *et al.* (2016). Evolutionary implications of C<sub>3</sub>-C<sub>4</sub> intermediates in the grass *Alloteropsis semialata*. *Plant, Cell Environ.*, 39, 1871–1873.
- McKown, A.D. & Dengler, N.G. (2007). Key innovations in the evolution of Kranz anatomy and C<sub>4</sub> vein pattern in *Flaveria* (Asteraceae). *Am. J. Bot.*, 94, 382–399.
- McKown, A.D. & Dengler, N.G. (2009). Shifts in leaf vein density through accelerated vein formation in C<sub>4</sub> *Flaveria* (Asteraceae). *Ann. Bot.*, 104, 1085–1098.
- McKown, A.D., Cochard, H. & Sack, L. (2010). Decoding leaf hydraulics with a spatially explicit model: principles of venation architecture and implications for its evolution. *Am. Nat.*, 175, 447–460.
- Nelson, T. (2011). The grass leaf developmental gradient as a platform for a systems understanding of the anatomical specialization of C<sub>4</sub> leaves. *J. Exp. Bot.*, 62, 3039–3048.
- Nelson, T. & Langdale, J.A. (1989). Patterns of leaf development in C<sub>4</sub> plants. *Plant Cell*, 1, 3–13.
- Olofsson, J.K., Bianconi, M., Besnard, G., Dunning, L.T., Lundgren, M.R., Holota, H. *et al.* (2016). Genome biogeography reveals the

- intraspecific spread of adaptive mutations for a complex trait. *Mol. Ecol.*, 25, 6107–6123.
- Renvoize, S.A. (1987). A survey of leaf-blade anatomy in grasses XI. Paniceae. *Kew. Bull.*, 42, 739–768.
- Ripley, B.S., Cunniff, J. & Osborne, C.P. (2013). Photosynthetic acclimation and resource use by the C<sub>3</sub> and C<sub>4</sub> subspecies of *Alloteropsis semialata* in low CO<sub>2</sub> atmospheres. *Glob. Change Biol.*, 19, 900–910.
- Sage, R.F., Christin, P.A. & Edwards, E.J. (2011). The C<sub>4</sub> plant lineages of planet Earth. *J. Exp. Bot.*, 62, 3155–3169.
- Sage, R.F., Khoshravesh, R. & Sage, T.L. (2014). From proto-Kranz to C<sub>4</sub> Kranz: building the bridge to C<sub>4</sub> photosynthesis. *J. Exp. Bot.*, 65, 3341–3356.
- Scarpella, E., Barkoulas, M. & Tsiantis, M. (2010). Control of leaf and vein development by auxin. *CSH Perspect. Biol.*, 2, a001511.
- Schlüter, U. & Weber, A.P. (2016). The road to C<sub>4</sub> photosynthesis: evolution of a complex trait via intermediary states. *Plant Cell Physiol.*, 57, 881–889.
- Schneider, C.A., Rasband, W.S. & Eliceiri, K.W. (2012). NIH Image to ImageJ: 25 years of image analysis. *Nat. Methods*, 9, 671–675.
- Scoffoni, C. & Sack, L. (2017). The causes and consequences of leaf hydraulic decline with dehydration. *J. Exp. Bot.*, 68, 4479–4496.
- Scoffoni, C., Albuquerque, C., Broderson, C.R., Townes, S.V., John, G.P., Bartlett, M.K. *et al.* (2017a). Outside-xylem vulnerability, not xylem embolism, controls leaf hydraulic decline during dehydration. *Plant Physiol.*, 173, 1197–1210.
- Scoffoni, C., Albuquerque, C., Broderson, C.R., Townes, S.V., John, G.P., Cochard, H. *et al.* (2017b). Leaf vein xylem conduit diameter influences susceptibility to embolism and hydraulic decline. *New Phytol.*, 213, 1076–1092.
- Sedelnikova, O.V., Hughes, T.E. & Langdale, J.A. (2018). Understanding the genetic basis of C<sub>4</sub> Kranz anatomy with a view to engineering C<sub>3</sub> crops. *Annu. Rev. Genet.*, 52, <https://doi.org/10.1146/annurev-genet-120417-031217>.
- Soros, C.L. & Dengler, N.G. (2001). Ontogenetic derivation and cell differentiation in photosynthetic tissues of C<sub>3</sub> and C<sub>4</sub> Cyperaceae. *Am. J. Bot.*, 88, 992–1005.
- Ueno, O. & Sentoku, N. (2006). Comparison of leaf structure and photosynthetic characteristics of C<sub>3</sub> and C<sub>4</sub> *Alloteropsis semialata* subspecies. *Plant, Cell Environ.*, 29, 257–268.
- Venables, W.N. & Ripley, B.D. (2002). *Modern Applied Statistics with S*, 4th edn. Springer, New York, USA.
- Wang, P., Khoshravesh, R., Karki, S., Tapia, R., Balahadia, C.P., Bandyopadhyay, A. *et al.* (2017). Re-creation of a key step in the evolutionary switch from C<sub>3</sub> to C<sub>4</sub> leaf anatomy. *Curr. Biol.*, 27, 3278–3287.
- Watcharamongkol, T., Christin, P.A. & Osborne, C.P. (2018). C<sub>4</sub> photosynthesis evolved in warm climates but promoted migration to cooler ones. *Ecol. Lett.*, 21, 376–383.
- Williams, B.P., Johnston, I.G., Covshoff, S. & Hibberd, J.M. (2013). Phenotypic landscape inference reveals multiple evolutionary paths to C<sub>4</sub> photosynthesis. *eLife*, 2, e00961.
- Wilson, J.T.R., Brown, R.H. & Windham, W.R. (1983). Influence of leaf anatomy on the dry matter digestibility of C<sub>3</sub>, C<sub>4</sub>, and C<sub>3</sub>/C<sub>4</sub> intermediate types of *Panicum* species. *Crop Sci.*, 23, 141–146.

## SUPPORTING INFORMATION

Additional supporting information may be found online in the Supporting Information section at the end of the article.

Editor, John Pannell

Manuscript received 29 October 2018

Manuscript accepted 31 October 2018